Catalysis Today 169 (2011) 16–23

Contents lists available at ScienceDirect

Catalysis Today

journal homepage: www.elsevier.com/locate/cattod

Characterization of iron cationic sites in ferrierite using Mössbauer spectroscopy

Edyta Tabor[a], Karel Závěta[b], Naveen K. Sathu[a], Zdeňka Tvarůžková[a], Zdeněk Sobalík[a,*]

[a] J. Heyrovský Institute of Physical Chemistry of the ASCR, v. v. i., Dolejškova 3, CZ-182 23 Prague 8, Czech Republic
[b] Joint Laboratory for Mössbauer Spectroscopy, Faculty of Mathematics and Physics, Charles University in Prague, V Holešovičkách 2, CZ-180 00 Prague 8, Czech Republic

ARTICLE INFO

Article history:
Available online 15 October 2010

Keywords:
Iron ferrierites
Cationic site
Mössbauer spectroscopy

ABSTRACT

Iron ferrierites with low iron content and well-defined cation occupation supported by FTIR, UV–vis and EPR analysis, were utilized in order to settle the Mössbauer parameters of individual iron cationic species. These samples thus could serve as standard for establishing parameters for the Mössbauer spectroscopy analysis. In accordance with the analysis and supported by the published DFT modeling iron ions were present in three types of cationic sites (one α and two β).

For the first time, experimental evidence supporting the proposed existence of two types of β sites for Fe(II) bonding has been presented. Fe(II) in two types of β sites were characterized by IS = 0.92 mm/s and QS = 0.44 mm/s, and IS = of 0.94 mm/s and QS = 0.70 mm/s. The Mössbauer parameters of the Fe(II) in α sites has been established with IS = 1.02 mm/s and QS = 2.02 mm/s.

1. Introduction

Iron zeolites are important redox catalysts with high potential for selective catalytic reduction of NO_x [1–3], partial oxidation of benzene to phenol [4,5], and direct decomposition of nitrous oxide [6–8]. Decomposition of nitrous oxide is highly important due to steadily increasing demands coming from new environmental legislation [9].

Recently, it was shown that iron ferrierite is superior to other iron zeolites, i.e. Fe-MFI, Fe-BEA, in N_2O decomposition activity, namely in the absence of NO [10]. The proposed structure, based on a high extent on DFT (Density Functional Theory) model of the active site includes the two irons in β cationic sites [10]. Accordingly, a direct experimental identification of the active site and detailed understanding of the structure of iron species in iron ferrierite is desirable.

The sitting of iron ions in iron ferrierites was described using FTIR spectroscopy. In accordance with previous findings for the position of divalent cations in pentasil zeolites, three different framework cationic sites (α, β, γ) for occupation by Fe(II) ions have been identified [11]. At low loadings (Fe/Al < 0.03), iron ions are located mostly in β sites. With increasing Fe loading, α and finally γ sites were gradually more populated. At high loadings (Fe/Al ~ 0.3), extra framework iron oxides were present as well [12]. The population of iron ions in different types of framework sites was shown to affect the catalytic activity of iron ferrierite in N_2O decomposition [11].

Recently, the information from FTIR measurements was extended by DFT calculations [13–15]. Sklenak et al. showed that bivalent iron ions exchanged into ferrierites can only form three stable configurations: α, β-1, and β-2 [15]. The β-1, and β-2 differ in the arrangement of Al atoms in the six-member ring. According to the DFT results, iron ions in α sites are located above the center of six-membered rings and coordinated to four oxygen atoms of the same ring. The most stable iron cation position is in the β-1 site, where iron ion is located in the plane of six-membered ring and coordinated to four oxygen atoms of the ring, and the O–Fe–O angle is 176°. The geometry of β-2 cationic site is similar to the geometry of β-1 position. Iron cations are in the plane of six-membered rings, bond to four oxygen atoms. The O–Fe–O angle is 172° due to different geometry of the β-2 site. The local deformation of the framework by bonding of iron cations in α or β positions, as well its oxidation states could be followed by FTIR. However, the difference in the local deformation of the ferrierite framework caused by β-1 or β-2 cannot be observed experimentally [14,15]. This technique also does not provide information on other forms of iron species, namely the oxidic ones.

Mössbauer spectroscopy is an ideal tool to study iron species in zeolites [16–19]. The advantage of Mössbauer spectroscopy is that there is no form of iron that is Mössbauer-silent [20]. The only limitation of Mössbauer spectroscopy is its sensitivity. Fe zeolites with relatively low Fe content (in the range below 1000–2000 ppm Fe) cannot be successfully analyzed, unless the samples with high enrichment by ^{57}Fe isotope are used [21]. Three main spectral parameters are used for the description of iron species: isomer shift, quadrupole splitting and magnetic hyperfine field. Isomer shift (IS) is providing information about the oxidation state of iron. Thus the value of isomer shift between 0.7 and 1.4 mm/s is assigned to Fe(II),

---

[*] Corresponding author. Tel.: +420 266053646; fax: +420 286582307.
E-mail address: zdenek.sobalik@jh-inst.cas.cz (Z. Sobalík).

0920-5861/$ – see front matter © 2010 Published by Elsevier B.V.
doi:10.1016/j.cattod.2010.09.017

whereas Fe(III) ions are characterized by isomer shift from 0.1 to 0.6 mm/s [16,22]. The reciprocal value of quadrupole splitting (QS) is proportional to the symmetry around iron ions. However, the value of quadrupole splitting is only indicative and the terms tetrahedral or octahedral coordination are used as crude approximation. One of the reasons is that there are many possible coordinations of iron in zeolites which are not included in the list of species typically used as Mössbauer standards. Moreover, the values of isomer shift and quadrupole splitting strongly depend on the primary and the secondary coordination ligands around the iron ions. Thus, very often the coordination of Fe is characterized as more or less asymmetric [22].

Majority of Mössbauer studies analyzing the iron centers in zeolites was focused on Fe-MFI. Panov et al. identified the formation of active α oxygen species formed after interaction with N_2O and stabilized on iron ions in MFI matrix ($Fe/Al \sim 0.1$). During this reaction the oxidation state of iron is changed from (II) to (III). Moreover, cationic binuclear hydroxide or μ-oxo bridged Fe complex were also proposed as active sites for N_2O decomposition [16].

In the case of steam-activated [Fe,Al]MFI with different iron concentrations (Fe/Al from 0.032 to 0.25) Taboada et al. have shown that most of iron is present as Fe(II) [20]. Analysis of Mössbauer data confirmed that nearly all Fe(II) present in investigated samples was oxidized at 350 °C by N_2O. Nevertheless, only a fraction of Fe(III) was able to generate active oxygen for the oxidation of benzene. It was shown that this fraction increased with decreasing iron concentration [20].

Overweg et al. [23] found that Fe(III) ions in isolated extraframework of MFI ($Fe/Al \sim 0.1$) sites and in small oxo-iron clusters are easily converted to Fe(II) species by thermal treatment at 350 °C and are oxidized back to Fe(III) by treatment in N_2O at 350 °C. Fe(III) in larger iron oxides did not reduce under these conditions [23].

The influence of different pretreatment procedures (calcination in air, evacuation or reduction by hydrogen) on the stability of Fe(III) in the lattice of BEA was reported by Lázár et al. [18]. The calcination of Fe-BEA led to the formation of mixed tetrahedral–octahedral Fe(III) (T_d/O_h) sites. After evacuation at 450 °C, auto reduction of Fe(III) to Fe(II) took place. Based on the Mössbauer parameters, authors assigned the individual structures to tetrahedral or octahedral coordination. However, this could apply to iron in oxo-species, but it could not be justified for the bivalent iron in the cationic sites [11].

Mauvezin et al. [24] used the Mössbauer spectroscopy to analyze the influence of the pretreatment on changes in iron sites in Fe-BEA as well. It was shown that after calcination in O_2 the iron ions were predominantly present as binuclear oxocations. The treatment with N_2O led to the formation of mononuclear and binuclear Fe-oxocations, which preferably formed in the samples with low Fe content [24].

Only few papers were focused on the characterization of iron ions in ferrierites by Mössbauer spectroscopy. Shevade et al. [25] studied the hydrothermal synthesis of Fe-FER. Deconvolution of Mössbauer spectra confirmed the isomorphous replacement of Al(III) by Fe(III) in the ferrierite structure. Mössbauer spectrum of the as-prepared Fe-FER (Fe/Al = 0.4) collected at room temperature showed a broad singlet with IS = 0.25 mm/s, which was assigned to Fe(III) in a tetrahedral coordination [25].

Lázár et al. studied the catalytic activity of the aluminoferrisilicate with ferrierite structure in oxidation of n-hexane and hydroxylation of phenol [26]. To specify the iron-containing catalytic sites in Al + Fe-FER, Mössbauer spectroscopy was employed. Mössbauer spectra of Al + Fe-FER (Fe/Al = 0.3) after calcination at 350 °C and measured at room temperature have shown that all iron ions were present as Fe(III). The Fe(III) sites in octahedral coordination were described by following parameters: IS = 0.37 mm/s, QS = 1.19 mm/s (62%) and IS = 0.35 mm/s, QS = 0.70 mm/s (32%). Fe(II) in tetragonal-octahedral coordination (coordination approaching tetrahedral symmetry of ligands) was characterized by IS = 0.95 mm/s, QS = 2.09 mm/s (5%). The evacuation of the sample led to an increase in symmetry around Fe ions; prevailing part (78%) of Fe(III) was observed in tetragonal coordination and the Fe(III) in octahedral coordination was not detected. After the treatment of Al + Fe-FER with hydrogen only 33% of iron was observed as Fe(III), the remaining part of iron was observed as Fe(II) in tetrahedral or octahedral coordination. Moreover, the presence of hypothetic $Fe_{lattice}$–O–$Fe_{extraframework}$ centers, which could play primary role in mild oxidation of n-hexane, was suggested.

Blasin-Aubé et al. measured the Mössbauer spectra of Fe-FER with lower concentration of iron (Fe/Al = 0.2). They used Mössbauer spectroscopy as a complementary method to FTIR spectroscopy to determine the oxidation state of iron in mononitrosyl complexes [27,28]. Deconvolution of Mössbauer spectrum of Fe-FER prepared by incipient wetness impregnation have shown that prevailing part (~90%) of iron hydrated sample was present as Fe(II) [27,28]. The Mössbauer spectrum of as-prepared Fe-FER measured at room temperature was decomposed into five components. Three of them corresponded to Fe(II): the first one had IS = 1.34 mm/s, QS = 1.49 mm/s (50%), the second one IS = 1.15 mm/s, QS = 2.35 mm/s (18%), and the third one IS = 1.02 mm/s, QS = 1.69 mm/s (16%). By FTIR spectra of adsorbed NO and CO these three types of species were identified as iron ions in framework positions. The component with high asymmetry, having QS = 3.42 mm/s with small spectral contribution (4%), was ascribed to iron cations located on the surface of Fe_2O_3 clusters. Finally, the component with IS = 0.59 mm/s and spectral contribution 12% corresponded to Fe_2O_3 [27,28].

Schwarze et al. [10] found 100% of Fe(II) in iron ferrierite with Fe/Al = 0.08 evacuated at 450 °C. The spectral analysis has shown that Fe(II) sites are characterized by IS = 0.94 mm/s, QS = 0.69 mm/s and IS = 1.18 mm/s, QS = 2.04 mm/s.

These literature data can be summarized as follows: in Mössbauer spectra of iron ferrierite with low iron content (Fe/Al = 0.08), two components characterized by IS = 0.94 mm/s, QS = 0.69 mm/s and IS = 1.18 mm/s, QS = 2.04 mm/s were found and assigned to Fe(II) [10]. In the case of iron ferrierite with Fe/Al = 0.2, majority of iron ions (90%) was observed as Fe(II) characterized by IS = 1.02 mm/s, QS = 1.69 mm/s; IS = 1.15 mm/s, QS = 2.35 mm/s, and IS = 1.34 mm/s, QS = 1.49 mm/s. About 10% of iron was observed as iron oxide [27,28]. The analysis of the results of Mössbauer measurements of iron ferrierite with Fe/Al = 0.3 have shown the presence of three types of Fe(III) described by following parameters: IS = 0.29 mm/s, QS = 0.56 mm/s; IS = 0.33 mm/s, QS = 1.34 mm/s, and IS = 0.36 mm/s, QS = 0.96 mm/s [26].

It can be concluded that the population of different types of iron species in iron ferrierite strongly depends on the amount of iron present in ferrierite. However, it is also clearly seen that there is no agreement on Mössbauer parameters of individual iron species in iron ferrierite and on the interpretation of their structure. Moreover, the nature of iron species and thus the values of isomer shift and quadrupole splitting depend on the conditions of measurement, especially temperature and presence of moisture or air. Therefore, the determination of Mössbauer parameters of well-defined iron species bonded in zeolite and under controlled conditions (high vacuum) seems to be desirable. The Mössbauer parameters determined in this way may be then used for the fitting of Mössbauer spectra of more complicated systems containing several iron species (e.g. in iron zeolite catalysts) in order to obtain reasonable results. It may be especially interesting for samples containing relatively high iron loading (Fe/Al = 0.2–0.3), where many forms of framework and extraframework iron species are present, which makes the interpretation of Mössbauer spectrum difficult.

Another interesting challenge is to find a correlation between the results obtained by Mössbauer spectroscopy and other techniques (FTIR and UV–vis spectroscopy or DFT calculations). Up to now, some iron species predicted theoretically were not confirmed by any experimental results. Also in this case, the preparation of iron ferrierites with well-defined location of iron ions may be beneficial. By measuring the samples pretreated by evacuation at high temperature (to reduce the influence of adsorbed water on the geometry of iron species), inherent Mössbauer parameters of individual iron species may be found. They can be then used to reconstruct the geometry and structure of iron sites in iron ferrierite.

The aim of this work was to identify the Mössbauer parameters of cationic iron species in iron ferrierites with very low iron content and thus containing only distinct iron species in well-defined positions. FTIR, UV–vis, and EPR spectroscopy was employed to support the interpretation of Mössbauer spectra. Thanks to carefully controlled experimental conditions, it was possible to distinguish the nature of several types of iron cationic species in iron ferrierites and establish their Mössbauer parameters and thus create a background for further analysis of samples containing complex mixtures of iron species, typical for iron-zeolites with higher iron content.

2. Experimental

2.1. Catalyst preparation

NH_4-FER (Tosoh, Japan; Si/Al = 8.6. The Na/K form was converted by repeating the ion exchange by NH_4NO_3 solution) was used as a parent material for the synthesis of iron ferrierites. Iron ions were introduced to the ferrierite structure using impregnation method described in details elsewhere [29]. Parent NH_4-FER was granulated into 0.3–0.6 mm grains and impregnated by acetylacetonate solution of $FeCl_3$ for 5 h. Then it was evacuated for 1 h at 100 °C, followed by evacuation at 350 °C for 3 h. After cooling, the sample was washed by distilled water and filtered, finally the organic content was removed by calcination in stream of air at 450 °C for 10 h than calcined in air flow at 420 °C for 10 h. In all syntheses, isotopically enriched $^{57}FeCl_3$ (prepared from iron oxide with ^{57}Fe enrichment over 96%; Isoflex, U.S.) was used. The samples of iron ferrierite with Fe/Al molar ratio of 0.018, 0.036, 0.072 and 0.30 were denoted as Fe-FER$_{0.018}$, Fe-FER$_{0.036}$, Fe-FER$_{0.072}$, and Fe-FER$_{>0.30}$, respectively.

2.2. Catalyst characterization

UV–vis spectra of dehydrated iron ferrierites in the range from 10 000 to 50 000 cm^{-1} were measured using a Perkin-Elmer Lambda 950 spectrometer equipped with Spectralon^{TM} integration sphere. Spectralon^{TM} was used as a reference. The spectra were recorded after dehydration of the sample at 450 °C for 3 h under vacuum (10^{-3} Pa). WinLab software was applied to recalculate spectra using the Schuster–Kubelka–Munk equation [30].

FTIR spectra of dehydrated iron ferrierites were measured with a resolution of 2 cm^{-1} at room temperature using a Nexus 670 FTIR (Thermo Nicolet) spectrometer. Before measurement of the spectra the sample is simultaneously dehydrated (at 450 °C) and evacuated (10^{-3} Pa) in a glass vacuum cell equipped with six position carousel holder and with NaCl windows.

The samples were prepared as self-supporting wafers having thickness between 5 and 10 mg/cm^2. The spectral intensities were normalized using the integral intensity area of the zeolite skeletal bands in the region between 1 750 and 2100 cm^{-1} for the standard sample thickness 5.5 mg/cm^2. The position of iron ions in the ferrierite cationic sites was monitored in the "skeletal transmission window" of FTIR spectrum (a region between 950 and 880 cm^{-1}), where the perturbed antisymmetric T–O–T stretching lattice vibrations induced by bonding of divalent ion were observed. The band position in transmission window was identified by a Fourier self-deconvolution procedure (OMNIC 4.1 software). Final data processing was carried out using the OriginPro 7.5 software (MicroLab Corporation, USA) [31,32] analyzing the spectra in the region of 960–880 cm^{-1}.

EPR spectra of dehydrated (at 450 °C for 3 h under vacuum (10^{-3} Pa)) iron ferrierites samples with low iron loading: Fe-FER$_{0.018}$, Fe-FER$_{0.036}$ were collected at room temperature with an ERS-220 spectrometer (Center for Production of Scientific Instruments, Academy of Sciences of GDR, Berlin, Germany) operated by a CU-1 unit (Magnettech, Berlin, Germany) in the X band. Mn^{2+} (g = 1.9860, MI = −1/2 line) was used as standard for g value determination.

For Mössbauer spectroscopy, self-supporting pellets of iron ferrierite were prepared by using a forming pressure of 5 MPa. A pellet having 10 mm in diameter and weight of ~100 mg was placed into a laboratory-made chamber that enabled thermal treating of the sample under various atmospheres and measuring of the spectra at room temperature under vacuum (10^{-3} Pa). The transmission ^{57}Fe Mössbauer spectra were collected in vacuum at room temperature after evacuation at 450 °C for 3 h using ^{57}Co in Rh matrix as a source. The maximum velocity of the source was 12 mm/s and the velocity scale was calibrated using α-Fe. The spectra were deconvoluted into Lorentzian-shaped components using MossWinn software. The components characterized by the corresponding Mössbauer parameters, i.e. isomer shift (IS), quadrupole splitting (QS), and magnetic hyperfine field (B_{hf}) were then assigned to individual iron species.

3. Results and discussion

3.1. FTIR spectra

FTIR spectra of dehydrated Fe-FER$_{0.018}$, Fe-FER$_{0.036}$, Fe-FER$_{0.072}$ and Fe-FER$_{>0.3}$ are presented in Fig. 1. The spectrum of Fe-FER$_{0.018}$ exhibits a strong band at 913 cm^{-1} and a weaker one at 935 cm^{-1}. It was shown by Wichterlová et al. [11] that with increasing iron concentration in ferrierites at first the β sites are occupied by Fe ions, while the other two cationic positions, α and γ sites, are occupied at higher iron concentrations.

The presence of iron in cationic sites is thus manifested by the formation of new bands in the "transmission window". The position of a band is specific for bare cation and its location; the intensity of these bands correlate with the cation content. Based on these literature data, the bands at 913 cm^{-1} and 935 cm^{-1} are assigned to iron ions in β and α cationic sites, respectively [11,17]. Due to principal similarity of these two bands, we assume that their extinction coefficients are similar, and their relative area would roughly reflect their relative concentration. Thus, prevailing part of iron ions (82%) in Fe-FER$_{0.018}$ is located in β cationic sites and only about 18% of present iron ions in Fe-FER$_{0.018}$ is sitting in α sites.

The analysis of FTIR spectrum of Fe-FER$_{0.036}$ provided two bands at 913 cm^{-1} and 935 cm^{-1} characteristic for Fe in β and α sites. In comparison with Fe-FER$_{0.018}$, the amount of Fe in β sites increased, but the relative concentration is lower (68%) and content of Fe in α sites increased to about 32%.

FTIR spectrum of Fe-FER$_{0.072}$ was deconvoluted into two bands at 913 cm^{-1} and 935 cm^{-1}. The skeletal bands at 913 cm^{-1} and 935 cm^{-1} are characteristic for Fe ions located in β and α cationic position, respectively. Quantitative analysis of the FTIR spectrum of Fe-FER$_{0.072}$ indicated that about 34% of iron ions are sitting in α cationic sites and 66% of Fe is located in β sites. Theses results

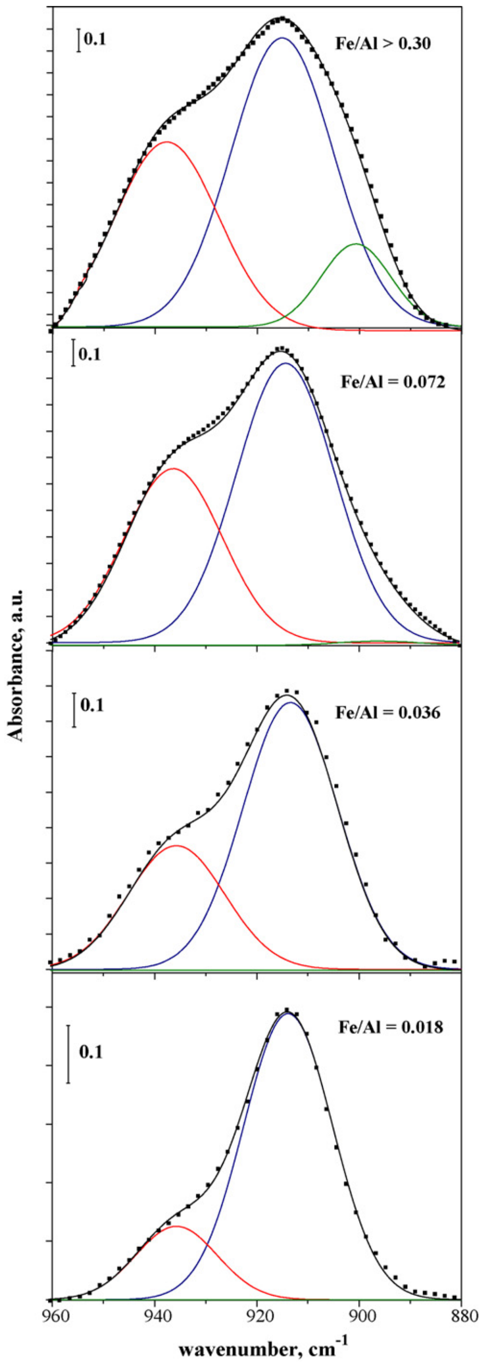

Fig. 1. FTIR spectra of dehydrated Fe-FER$_{0.018}$, Fe-FER$_{0.036}$, Fe-FER$_{0.072}$ and Fe-FER$_{>0.30}$. Deconvolution of the infrared spectra at the T–O–T region of the dehydrated Fe-FER$_{0.018}$, Fe-FER$_{0.036}$, Fe-FER$_{0.072}$ and Fe-FER$_{>0.30}$ with different Fe content after evacuation for 4 h at 450 °C. (■) experimental data, (🟥) α site, (🟦) β site and (🟩) γ site. (For interpretation of the references to colour in this figure legend, the reader is referred to the web version of the article.)

confirmed that the higher amount of iron in Fe-FER the higher amount of iron in α sites is observed.

The spectrum of Fe-FER$_{>0.30}$ revealed the presence of bands at 913 cm^{-1} and 935 cm^{-1} as well, and a weak band at 897 cm^{-1} was observed, which could be assigned to iron ions in γ cationic sites. Accordingly, by increasing the iron content the amount of iron located in α sites increased to about 36%, but more than half of iron (54%) is present in β sites, and 10% of iron is observed in γ sites.

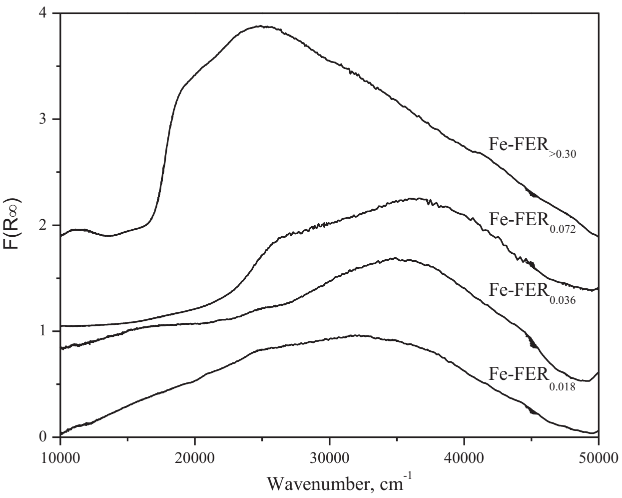

Fig. 2. UV–vis spectra of dehydrated Fe-FER$_{0.018}$, Fe-FER$_{0.036}$, Fe-FER$_{0.072}$ and Fe-FER$_{>0.30}$. The spectra of Fe-FER$_{0.018}$ and Fe-FER$_{0.036}$, were folded 40 times; the spectrum Fe-FER$_{0.072}$ was folded 15 times.

Thus, the three samples with 0.018, 0.036 and 0.072 Fe/Al ratio present specimens with basically different ratio between iron occupation in the three cationic positions and could serve as the standards for the Mössbauer study. The sample with high iron concentration, i.e. Fe/Al > 0.30 is above the limit of iron concentration for prevailing occupation of the cationic sites and, as shown later, also contains large proportion of iron oxide species.

3.2. UV–vis spectra

The UV–vis spectra of dehydrated at 450 °C Fe-FER$_{0.018}$, Fe-FER$_{0.036}$, Fe-FER$_{0.072}$ and Fe-FER$_{>0.30}$ are presented in Fig. 2. All spectra exhibited bands at 45 600 cm^{-1}, 37 800 cm^{-1}, and 34 000 cm^{-1}, which can be assigned to Fe(III)O or Fe(II) charge transfer [17,20]. The additional absorption band at 15 000 cm^{-1}observed in UV–vis spectrum of Fe-FER$_{0.036}$ may be assigned to Fe(II) in different than planar coordination [33]. The band at 28 200 cm^{-1}, which indicated the presence of Fe(III) in the sample, is present in the spectrum of Fe-FER$_{0.072}$. This band is characteristic for C-T transition Fe(III) [30]. The spectra of Fe-FER$_{>0.30}$ are more complex. At first, additional bands at 11 000 cm^{-1} and 11 800 cm^{-1} can be seen. These bands may correspond to d–d transitions of Fe(III) in octahedral environment of oxygen-containing ligands, indicating the presence of extra-framework clusters of hematite [30,33]. Secondly, the strong absorption edge is visible at 18 500 cm^{-1}, which can be ascribed to electron pair transition typical for Fe(III) ions in hematite. All these additional bands, which are not present in the spectra of Fe-FER$_{0.018}$, Fe-FER$_{0.036}$, and Fe-FER$_{0.072}$, confirm the presence of extra framework iron oxides in Fe-FER$_{>0.30}$. From the position of this band, the particle size of hematite can be estimated to be in the order of tenths of nanometers.

In the UV–vis spectra of both Fe-FER$_{0.072}$, and Fe-FER$_{>0.30}$ the band centered at 27 000 cm^{-1} is present, this band can be assigned to Fe(III) oxo species [34].

Thus, according to the UV–vis results only the samples with very low iron content, i.e. Fe-FER$_{0.018}$, Fe-FER$_{0.036}$, are after dehydration at 450 °C free of the Fe(III) species, while in both the samples with higher iron content, i.e. Fe-FER$_{0.072}$, and even more in Fe-FER$_{>0.30}$, additional species containing Fe(III) are present. The iron cluster were evidenced only in the samples with the higher iron loading Fe-FER$_{>0.30}$.

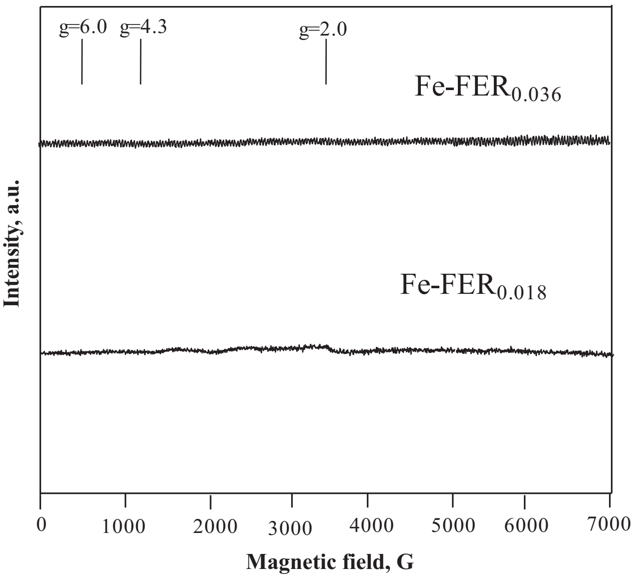

Fig. 3. EPR spectra of dehydrated Fe-FER$_{0.018}$, Fe-FER$_{0.036}$.

3.3. *EPR spectra*

EPR spectroscopy is able to identify the paramagnetic species at the ppm level. In order to confirm the absence of trivalent form of iron in the samples with low iron content, EPR spectra of dehydrated Fe-FER$_{0.018}$ and Fe-FER$_{0.036}$ were measured (Fig. 3). In accordance with the literature data the appearance of the signal line in EPR spectra of iron zeolites at g = 6.0, 4.3, and 2.0 are assigned to paramagnetic Fe(III) ions in extra-framework position, isolated Fe(III) in T_d coordination, and Fe$_x$O$_y$ oligomers or oxide species, respectively [11,5].

In the EPR spectra of dehydrated Fe-FER$_{0.018}$ and Fe-FER$_{0.036}$ any of the above listed signals characteristic for paramagnetic Fe(III) species were not observed. Therefore, it can be concluded that in dehydrated Fe-FER$_{0.018}$ and Fe-FER$_{0.036}$ the iron oxide clusters were not present.

3.4. *Mössbauer spectra*

The Mössbauer spectra of dehydrated Fe-FER$_{0.018}$, Fe-FER$_{0.036}$, Fe-FER$_{0.072}$ and Fe-FER$_{>0.30}$ as well as their fits are shown in Figs. 4–7. The corresponding parameters of the Mössbauer spectra are collected in Table 1.

From FTIR, UV–vis, and EPR spectra of dehydrated Fe-FER$_{0.018}$ it was concluded that only Fe(II) ions located in cationic positions are present in this sample (Figs. 1–3), while the FTIR data further indicate Fe(II) location in the β and α positions with relative occupation $\beta \gg \alpha$. Nevertheless, deconvolution (of Mössbauer spectrum of Fe-FER$_{0.018}$) into two components exhibited high value of χ^2, while the addition of another component significantly improved the quality of the fit. The deconvolution of Mössbauer spectrum of dehydrated Fe-FER$_{0.018}$ into three components is shown in Fig. 4. Owing to the isomer shift higher than 0.7 mm/s, all the three components were ascribed to Fe(II) ions in cationic sites of ferrierite framework [11]. Assignment of the obtained results would thus take into consideration the relative concentration ratio obtained by FTIR results and additionally the results of structural analysis of the Fe-FER provided by periodic DFT studies [14,15]. Benco et al. have shown that α sites possess lower symmetry than β sites [13,14]. As it is known that for Fe(II) ions the value of quadrupole splitting is reciprocally proportional to the symmetry of the iron centers [16,35], the component with the highest quadrupole splitting was attributed to Fe(II) ions

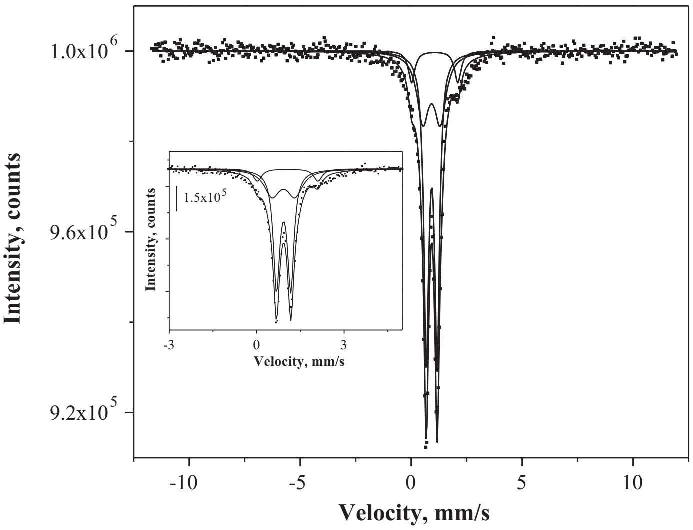

Fig. 4. Mössbauer spectrum of dehydrated Fe-FER$_{0.018}$ together with its fits.

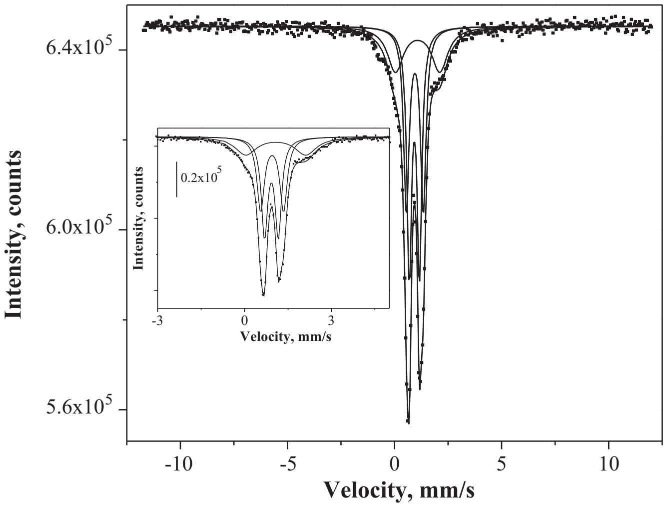

Fig. 5. Mössbauer spectrum of dehydrated Fe-FER$_{0.036}$ together with its fits.

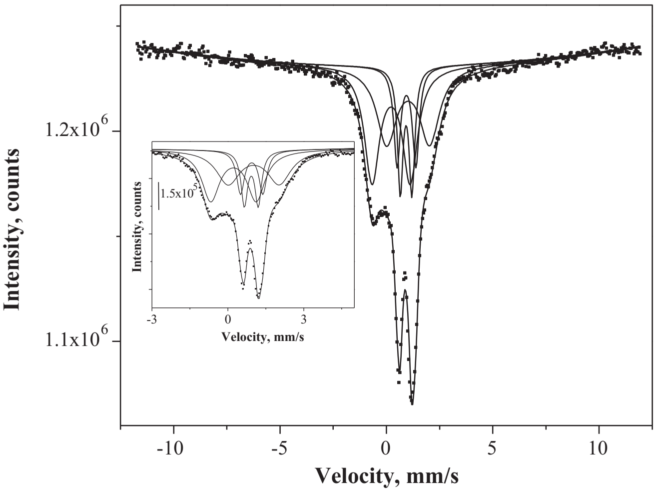

Fig. 6. Mössbauer spectrum of dehydrated Fe-FER$_{0.072}$ together with its fits.

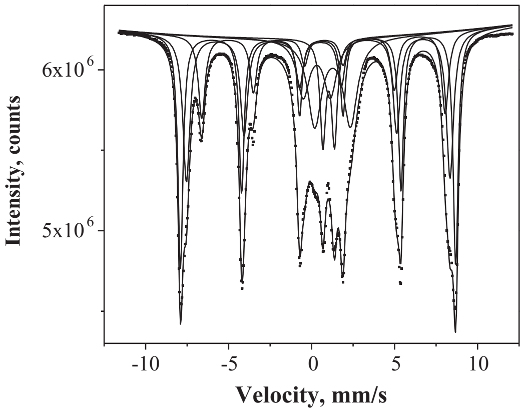

Fig. 7. Mössbauer spectrum of dehydrated Fe-FER$_{>0.30}$ together with its fits.

in α sites, i.e. a site with lower symmetry where the iron cation is situated above the plane containing the liganding oxygen atoms. The amount of α sites estimated by Mössbauer spectroscopy (18%) is in accordance with the semiquantitative estimation from the FTIR spectra (17%). The other two components with lower values of quadrupole splitting were ascribed both to Fe(II) ions in β sites. The presence of two types of β sites, differing in the arrangement of Al atoms in the six-membered ring was earlier predicted by quantum chemistry calculations [13,14]. However, to the best of our knowledge, they were not experimentally verified up to now.

These two types of β sites (β-1 and β-2) could be distinguished thanks to the difference in the arrangement of the Al pair in the six-membered ring of the β site which would be manifested in the Mössbauer spectra while it would not be noticed in the relatively broad infrared bands. Based on quantum chemical calculations, it was suggested that coordination of iron ions in both β sites is similar, with iron in β-1 and β-2 sites directly in the plane of six-membered ring of ferrierite and coordinated to four oxygen atoms of these ring [14,15]. This is in agreement with the values of quadrupole splitting (0.44 mm/s and 0.70 mm/s), which in both identified structures correspond to coordination number four [26,36]. On the other hand, the difference in the values of quadrupole splitting between these two types (0.44 and 0.70 mm/s) of β sites could be correlated with the slightly different symmetry of individual iron species [26,37,38].

Therefore, it can be concluded that the two types of β sites exhibit, in accordance with the DFT model [15], slightly different geometry. In accordance with these arguments, the β-1 site should exhibit smaller deformation and thus higher symmetry and could be assigned to the component characterized by IS = 0.92 mm/s; QS = 0.44 mm/s. The component with the Mössbauer parameters IS = 0.94 mm/s; QS = 0.70 mm/s would then be assigned to β-2 site, the site with slightly lower symmetry. These assignments of the Mössbauer components to the individual β sites are only tentative as they are only based on the evaluation of the DFT predicted structures of the local geometry of the β sites.

As shown by the DFT calculations [15], the coordination of iron ions in α sites is different, i.e. the iron ions are coordinated to four bridging oxygens of the framework but are located above the plane of six-membered rings of the ferrierite framework [15]. In accordance with this structure, the environment of iron ions in α sites displays lower symmetry than that of iron ions in β sites and the value of quadrupole splitting is considerably higher (Table 2). Accordingly, assignment of the Mössbauer (IS = 1.02 mm/s; QS = 2.02 mm/s) signal to Fe(II) in α position is well established.

From Table 2 it is seen that the Mössbauer parameters of iron species in Fe-FER$_{0.018}$ are different from that reported in literature (Table 2). It is due to the fact that the majority of Mössbauer studies were focused on iron ferrierites with much higher iron content, i.e. with Fe/Al > 0.1 [25–28]. This high concentration of iron led to the formation of several types of iron species and therefore complex Mössbauer spectra arose. Consequently, the fitting procedure was difficult and the components obtained could be hardly ascribed to individual iron species (Table 2, [25–28]). Moreover, the Mössbauer spectra were mostly collected for fully hydrated samples and exposed to air atmosphere [25–28]. In the case of Fe(II) ions the strong adsorption of water molecules lowered the symmetry around iron ions, and resulted in higher values of quadrupole splitting (Table 2, [25–28]).

In order to obtain the real values of Mössbauer parameters of iron cation without any extraframework ligand, it is necessary to perform the measurements after high temperature vacuum treatment and collect the spectra under vacuum. Moreover, the low concentration of iron in our samples would eliminate the signals of additional iron non-cationic species and help to precisely distinguish individual iron species. The advantage of this approach was confirmed by Jíša et al. [10], using the vacuum of about 10^{-1} Pa during the accumulation of the spectra. In the present work better evacuation system is used which provide for collection of the spectra under better vacuum (10^{-3} Pa) during the whole experiment and elimination of the formation of the extra-framework ligands over Fe(II) sites. Under such conditions quite long spectra collection could have been realized (over

Table 1
The parameters of the Mössbauer spectra of dehydrated Fe-FER$_{0.018}$, Fe-FER$_{0.036}$, Fe-FER$_{0.072}$, and Fe-FER$_{>0.30}$.

Catalyst	Isomer shift (mm/s)	Quadrupole splitting (mm/s)	B_{hf} (T)	Spectral contribution (%)	Oxidation state and coordination of Fe ions
Fe-FER$_{0.018}$	0.92	0.44		41	Fe(II)
	0.94	0.70		42	Fe(II)
	1.02	2.02		17	Fe(II)
Fe-FER$_{0.036}$	0.92	0.45		31	Fe(II)
	0.94	0.73		44	Fe(II)
	1.02	2.06		25	Fe(II)
Fe-FER$_{0.072}$	0.92	0.46		6	Fe(II)
	0.94	0.71		29	Fe(II)
	1.02	2.02		32	Fe(II)
	0.30	1.87		33	Fe(III)
Fe-FER$_{>0.30}$	0.41		50.0	15	γ-Fe_2O_3 [B]
	0.28		47.20	36	γ-Fe_2O_3 [A]
	0.35	−0.21	50.48	14	α-Fe_2O_3
	1.09	2.02		14	Fe(II)
	1.02	0.71		8	Fe(II)
	0.20	1.69		8	Fe(III)

Table 2
Mössbauer parameters of iron ferrierites from the literature.

Catalyst	Isomer shift (mm/s)	Quadrupole splitting (mm/s)	Spectral contribution (%)	Oxidation state of Fe ions	Reference
Fe/Al = 0.4; hydrated	0.25	[a]	100	Fe(III)Td	[25]
Fe/Al = 0.3 hydrated	0.37	1.19	62	Fe(III)Oh	[26]
	0.35	0.70	32	Fe(III)Oh	
	0.95	2.09	5	Fe(II)Td/Oh	
Fe/Al = 0.3 dehydrated	0.27	1.88	78	Fe(III)Td	[26]
	0.89	0.58	13	Fe(II)Oh	
	1.04	2.27	9	Fe(II)Oh/Td	
Fe/Al = 0.2[b] hydrated	1.34	1.49	50	Fe(II)	[27,28]
	1.15	2.35	18	Fe(II)	
	1.02	1.69	16	Fe(II)	
	1.20	3.42	4	Fe(II)	
	0.59	3.00	12	Fe$_2$O$_3$	

[a] Assuming singlet signal.
[b] Prepared by ion exchange with the Mohŕsalt.

70 h) and accordingly high quality spectra even for samples with very low iron content and with potential for detail analysis were obtained.

The analysis of Mössbauer spectrum of dehydrated Fe-FER$_{0.036}$ presented in Fig. 5 provided three components. Their isomer shifts and quadrupole splitting are practically the same as in the case of Fe-FER$_{0.018}$. Therefore, they were ascribed to Fe(II) ions in α sites and the two types of β sites. In comparison with Fe-FER$_{0.018}$, the Fe-FER$_{0.036}$ sample has two times higher Fe loading and consequently the population of iron species is different. Whereas the spectral contribution of iron in β sites decreased from 83% to 75%, the spectral contribution of iron in α sites increased from 17% to 25%. These results are in agreement with the general tendency deduced from the FTIR experiments, showing preference for β sites occupation and increasing population of α sites with increasing Fe content.

Mössbauer spectrum of dehydrated Fe-FER$_{0.072}$ (Fig. 6) was fitted by 4 components. Three of them were assigned to Fe(II) and one to Fe(III). Components corresponding to Fe(II) exhibit similar values of IS and QS as Fe(II) ions in Fe-FER$_{0.018}$ and Fe-FER$_{0.036}$. In the case of Fe-FER$_{0.072}$, the spectral contribution of the component characterized by Mössbauer parameters IS = 0.92 mm/s; QS = 0.46 mm/s decreased with increasing iron content. The component described by Mössbauer parameters IS = 1.02 mm/s; QS = 2.02 mm/s was assigned to iron in cationic sites. The amount of Fe(II) located in α sites is 41%.

This corroborates the results from FTIR spectroscopy: the amount of Fe located in α cationic sites is increasing with increasing iron concentration while the concentration of β sites is relatively decreasing. Analysis of the spectral contribution of components assigned to Fe(II) showed that with the increasing Fe concentration the spectral contribution of components assigned to Fe(II) in β-1 cationic site relatively decreases. In the case of the sample with the lowest iron content, i.e. the samples with Fe-FER$_{0.018}$, population of iron β-1 and β-2 sites is roughly equal. By increasing the iron content, the relative proportion of β-1 in β sites is decreasing and the β-2 site highly prevail at samples with Fe/Al over 0.072. We assume that the β-1 position is saturated already at low iron concentration, and these present thus less than 6% of the β sites.

Additional Fe(III) species, observed in sample with Fe/Al = 0.072 is characterized by IS = 0.30 mm/s and QS = 1.87 mm/s. It could not be probably assigned to isolated iron in cationic positions, nevertheless the Mössbauer parameters are still consistent with Fe(III) in tetrahedral coordination [26]. In accordance with the UV–vis results we tentatively propose assignment of the component with IS = 0.30 mm/s and QS = 1.87 mm/s its interpretation as Fe(III) dinuclear complex which is not decomposed during evacuation at 450 °C or as isolated extra framework Fe(III) ions [22,38].

In accordance with the UV–vis results, Mössbauer spectrum of dehydrated Fe-FER$_{>0.30}$ (Fig. 7) revealed the presence of high amount of extra framework iron oxides. The component described by IS = 0.35 mm/s; B_{hf} = 50.48 T is characteristic for hematite [35,37]. Besides hematite, maghemite was observed as well. The component described by IS = 0.41 mm/s; B_{hf} = 50.0 T is characteristic for the octahedral [B] sites and the other one with IS = 0.28 mm/s; B_{hf} = 47.20 T correspond to the tetrahedral [A] sites of the maghemite structure. Extra framework iron oxides represent the major type (>50%) of iron species in Fe-FER$_{>0.30}$.

Apart from these oxides, two doublets corresponding to iron ions in cationic position of ferrierite were observed. The doublets with IS = 1.09 mm/s; QS = 2.02 mm/s and IS = 1.02 mm/s; QS = 0.71 mm/s can be ascribed, as in samples with much lower iron content, to Fe(II) in cationic position, α and β-2 respectively. Nevertheless, the speciation of iron in cationic positions in Fe-FER$_{>0.30}$ cannot be reliably quantified because of several overlapped components arising from iron oxides. Finally, the doublet with fitting parameters IS = 0.20 mm/s; QS = 1.69 mm/s is characteristic for tetrahedrally coordinated Fe(III), attributed tentatively to dinuclear Fe(III) complex either to isolated extra framework Fe(III) ions or to small particles of iron oxides. The differences in values of fitting parameters describing iron ions in framework positions can be explained by the formation of framework – extra-framework dinuclear Fe$_{\mathrm{FW}}$–O–Fe$_{\mathrm{EFW}}$ species [22,39]. Mössbauer spectrum of dehydrated Fe-FER$_{>0.30}$ confirmed that the introduction of high amount of iron leads to the formation samples with very complex mixture of iron species, including several types of iron oxides in various stages of development [2].

4. Conclusions

As evidenced by combined FTIR, UV–vis, EPR, and Mössbauer spectroscopy, Fe-FER with very low content of iron (Fe/Al < 0.1) contains negligible amount of oxidic species and the prevailing part of Fe is present in the form of divalent cations. These conclusions are in line with previous results predicting for such low content of divalent cations high preference to the occupation of the cationic positions. Accordingly, the iron ferrierites samples with low Fe/Al molar ratio (0.018 and 0.036) prepared by impregnation method contained exclusively Fe(II) ions. In accordance with the general tendency of the prevailing occupation of the β positions of zeolite at low level of exchange, the occupation of the α position in both samples represent a minority. In agreement with this known general tendency, the β site is manifested as the majority cation position occupied by divalent iron ion in the FTIR results. The relative occupation of β sites decreases in the samples with higher iron content and the α occupation increases up to about 50% of all cationic iron sites in the sample with Fe/Al of 0.72. The FTIR results are in agreement with the predominant occupation of β cationic sites, which constitute over 80% of the iron present in the sample with the lowest iron content; population of α sites was increasing with increasing iron content. The introduction of high amount of iron (Fe/Al = 0.30) into ferrierite structure led to formation of extra framework iron oxides and results in very complex Mössbauer profiles which could not be reliably analyzed by the used fitting procedure. This Fe/Al over 0.3 is approaching the limiting capacity of the used ferrierite with Si/Al ~9 to bond divalent cations.

Accordingly, it could be concluded that the three samples of Fe-FER with Fe/Al of 0.018, 0.036 and 0.072 provide a standard for reliable establishment of the Mössbauer parameters of iron cations in the cationic positions, and bring the first experimental support for the existence of two types of β sites in iron ferrierite. Moreover, it also suggests that the presence of the two types of β sites in the given ferrierite is not equal and one of them is saturated by iron cations already at Fe/Al ratio of ~0.05. We do not succeed in identification of the parameters of the Fe(II) in γ position, which is occupied only in samples with high amount of iron oxide species which makes the spectra analysis for the minority components unreliable.

Accordingly, the established Mössbauer parameters for isolated iron cations and their assignment could be summarized as follows:

β cationic sites:

- assigned tentatively to β-1: IS = 0.92 mm/s and QS = 0.44 mm/s,
- assigned tentatively to β-2: IS = 0.94 mm/s and QS = 0.70 mm/s.

α cationic site:

IS = 1.02 mm/s and QS = 2.02 mm/s.

Acknowledgments

This work was financially supported by the Grant Agency of the Academy of Sciences of the Czech Republic (Project No. KAN100400702), the Grant Agency of the Czech Republic (Project No. 203/09/1627), Center of Excellence IDECAT NMP3-CT-2005-011730, and MSMT CR project VZ 0021620834.

References

[1] A.L. Kustov, T.W. Hansen, M. Kustova, C.H. Christensen, Appl. Catal. B 76 (2007) 311.
[2] L. Čapek, L. Vradman, P. Sazama, M. Herskowitz, B. Wichterlová, R. Zukerman, R. Brosius, J.A. Martens, Appl. Catal. B 70 (2007) 53.
[3] A.M. Frey, S. Mert, J. Due-Hansen, R. Fehrmann, C.H. Christensen, Catal. Lett. 130 (2009) 1.
[4] L.V. Pirutko, V.S. Chernyavsky, A.K. Uriarte, G.I. Panov, Appl. Catal. A 227 (2002) 143.
[5] A. Ribera, I.W.C.E. Arends, S. de Vries, J. Pérez-Ramírez, R.A. Sheldon, J. Catal. 195 (2000) 287.
[6] J. Pérez-Ramírez, J. Catal. 227 (2004) 512.
[7] I. Melian-Cabrera, C. Mentruit, J.A.Z. Pieterse, R.W. van den Brink, G. Mul, F. Kapteijn, J.A. Moulijn, Catal. Commun. 6 (2005) 301.
[8] M. Mauvezin, G. Delahay, B. Coq, S. Kieger, J.C. Jumas, J. Olivier-Fourcade, J. Phys. Chem. B 105 (2001) 928.
[9] http://ec.europa.eu/environment/climat/emission/pdf/2nd_phase/final_opt_in_decision_at.pdf.
[10] K. Jíša, J. Nováková, M. Schwarze, A. Vondrová, S. Sklenák, Z. Sobalík, J. Catal. 262 (2009) 27.
[11] B. Wichterlová, Z. Sobalík, J. Dědeček, Appl. Catal. B 41 (2003) 97.
[12] M. Rauscher, R. Mönnig, K. Kesore, W. Schwieger, A. Tissler, T. Turek, Appl. Catal. A 84 (1999) 249.
[13] L. Benco, T. Bucko, R. Grybos, J. Hafner, Z. Sobalik, J. Dedecek, J. Hrusak, J. Phys. Chem. C 111 (2007) 586.
[14] L. Benco, T. Bucko, R. Grybos, J. Hafner, Z. Sobalik, J. Dedecek, S. Sklenak, J. Hrusak, J. Phys. Chem. C 111 (2007) 9393.
[15] S. Sklenak, P.C. Andrikopoulos, B. Boekfa, B. Jansang, Jana Nováková, L. Benco, T. Bucko, J. Hafner, J. Dědeček, Z. Sobalík, J. Catal. (2010), doi:10.1016/j.jcat.2010.04.008.
[16] K.A. Dubkov, N.S. Ovanesyan, A.A. Shteinman, E.V. Starokon, G.I. Panov, J. Catal. 207 (2002) 341.
[17] M. Schwarze, Z. Sobalik, Z. Tvarůžková, E.G. Caspary, D. Nižnanský, Czechoslovak J. Phys. 56 (Suppl. E) (2006) E147.
[18] A. Raj, S. Sivasanker, K. Lázár, J. Catal. 147 (1994) 207.
[19] P. Fejes, J.B. Nagy, J. Halasz, A. Oszko, Appl. Catal. A 175 (1998) 89.
[20] J.B. Taboada, E.J.M. Hensen, I.W.C.W. Arends, G. Mul, A.R. Overweg, Catal. Today 110 (2005) 221.
[21] P. Fejes, J.B. Nagy, K. Lázár, Appl. Catal. A Gen. 190 (2000) 117.
[22] K. Lázár, O. Pozdnyakova, A. Wootsch, P. Fejes, Hyperfine Interact. 167 (2006) 779.
[23] A.R. Overweg, M.W.J. Craje, A.M. van der Kraan, I.W.C.E. Arends, A. Ribera, R.A. Sheldon, J. Catal. 223 (2004) 262.
[24] M. Mauvezin, G. Delahay, B. Coq, S. Kieger, J.C. Jumas, J. Olivier-Fourcad, J. Phys. Chem. B 105 (2001) 928.
[25] S. Shevade, R.K. Ahedi, A.N. Kotasthane, Catal. Lett. 49 (1997) 69.
[26] K. Lázár, G. Lejeune, R.K. Ahedi, S.S. Shevade, A.N. Kotashane, J. Phys. Chem. B 102 (1998) 4865.
[27] E. Ivanova, M. Mihaylov, K. Hadjiivanov, V. Blasin-Aubé, O. Marie, A. Plesniar, M. Daturi, Appl. Catal. B, Environ. (2008), doi:10.1016/j.apcatb.2009.10.006.
[28] V. Blasin-Aubé, O. Marie, J. Saussey, A. Plesniar, M. Daturi, N. Nguyen, C. Hamon, M. Mihaylov, E. Ivanova, K. Hadjiivanov, J. Phys. Chem. C 113 (2009) 8387.
[29] CZ 293917 B6 (2001).
[30] L. Čapek, V. Kreibich, J. Dědeček, T. Grygar, B. Wichterlová, Z. Sobalík, J.A. Martens, R. Brosius, V. Tokarová, Micropor. Mesopor. Mater. 80 (2005) 279.
[31] Z. Sobalík, J. Dědeček, D. Kaucký, B. Wichterlová, L. Drozdová, R. Prins, J. Catal. 194 (2000) 330.
[32] Z. Sobalík, Z. Tvarůžková, B. Wichterlová, Micropor. Mesopor. Mater. 25 (1998) 225.
[33] J.-P. Lange, K. Klier, Zeolites 14 (1994) 462.
[34] G.D. Pirngruber, P.K. Roy, R. Prins, Phys. Phys. Chem. Chem. Phys. 8 (2006) 3939.
[35] T. Grygar, J. Dědeček, P.P. Kruiver, M.J. Dekkers, P. Bezdička, O. Schneeweiss, Catena 53 (2003) 115.
[36] E. Kuzmann, S. Nagy, A. Vértes, Pure Appl. Chem. 75 (2003) 801.
[37] R.G. Burns, Hyperfine Interact. 9 (1994) 739.
[38] K. Závěta, A. Lančok, M. Maryško, E. Pollert, D. Horák, Czechoslovak J. Phys. 56 (Suppl. E) (2006) E83.
[39] P. Fejes, I. Kiricsi, K. Lázár, I. Marsi, A. Rockenbauer, L. Korecz, J. Nagy, R. Aiello, F. Testa, Appl. Catal. B 242 (2003) 247.